

SAGA-HE-98-96

May 8, 1996

Parton Distributions in Nuclei: Overview and Prospect

S. Kumano *

Department of Physics
Saga University
Saga 840, Japan

Invited talk given at the Workshop on
“New Developments in QCD and Hadron Physics”
Kyoto, Japan, Jan.22-24, 1996 (talk on Jan.23, 1996)

* Email: kumanos@cc.saga-u.ac.jp. Information on his research is available at <http://www.cc.saga-u.ac.jp/saga-u/riko/physics/quantum1/structure.html> or at <ftp://ftp.cc.saga-u.ac.jp/pub/paper/riko/quantum1>.

Parton Distributions in Nuclei: Overview and Prospect

S. Kumano *

Department of Physics, Saga University
Honjo-1, Saga 840, Japan

Abstract

We give a brief overview of nuclear parton distributions. First, the EMC effect is discussed together with possible interpretations such as nuclear binding and Q^2 rescaling. Next, we explain shadowing descriptions: vector-meson-dominance-type and parton-recombination models. Nuclear dependence of Q^2 evolution should be interesting in testing whether or not DGLAP equations could be applied to nuclear structure functions. Status of nuclear sea-quark and gluon distributions is discussed. The structure function b_1 , which will be measured at HERMES and possibly at ELFE, could shed light on a new aspect of high-energy spin physics.

1 Introduction

From the early SLAC experiments on electron scattering, nuclear targets have been used just as a tool for measuring nucleon structure functions. Nuclear corrections are not taken seriously in 1970's except for apparent nucleon-Fermi-motion corrections. Nucleons are bound in a nucleus with average binding energy 8 MeV and typical momentum 200 MeV. These are fairly small compared with reaction energy of several GeV or more in electron or muon scattering. For this reason, nuclear environment was not expected to alter nucleon properties significantly. Even though signature of nuclear modification in the F_2 structure function is found in the SLAC data in 1970's, they are not studied extensively. On the other hand, the European Muon Collaboration (EMC) took the topic rather seriously and published the first paper in 1983 [1]. The nuclear modification of F_2 is now known as the (old) EMC effect.

In the mid 1980's, there are many theoretical publications on this topic, in particular on medium and large x physics. We cannot list all of the ideas in this paper. A conservative one is to interpret it in term of nuclear binding and Fermi motion [2]. On the other hand, there is another extreme model, Q^2 rescaling [3]. In contrast to the binding model in which bound nucleon F_2 is the same as the free one, it is modified due to nuclear environment. The details of these models are discussed in section 2.

From the late 1980's, nuclear F_2 structure functions in the shadowing region ($x < 0.1$) are investigated in detail experimentally and theoretically. In particular, accurate New Muon Collaboration (NMC) data make it possible to test theoretical shadowing models. The traditional idea of describing the shadowing is a vector-meson-dominance

(VMD) model. The virtual photon transforms into vector-meson states, which interact with the target nucleus. The VMD contribution decreases as $1/Q^2$ at large Q^2 , so various extensions of the model ($q\bar{q}$ continuum, Pomeron exchange) are studied. On the other hand, there exists an infinite-momentum interpretation in terms of parton recombinations, which are parton interactions from different nucleons in the nucleus. Shadowing phenomena are discussed in section 3. Comments on sea-quark and gluon distributions are also given.

Bjorken scaling works roughly for structure functions, and Q^2 dependence is a small effect. It is inevitably difficult to find nuclear effects within the small Q^2 variation. However, the nuclear dependence is recently found in a NMC experiment [4] by measuring tin and carbon Q^2 variation differences. The data are interesting in testing whether or not DGLAP equations could be applied to the nuclear case. This topic is discussed in section 4.

High-energy spin physics becomes a very popular topic since the EMC discovery of proton-spin “crisis”. In order to investigate a new field of spin physics, structure of the spin-one deuteron is currently under investigation by HERMES. It is expected that a new spin field is explored in the near future. Major features of the structure function b_1 are discussed in section 5.

2 Nuclear modification of F_2 at medium x

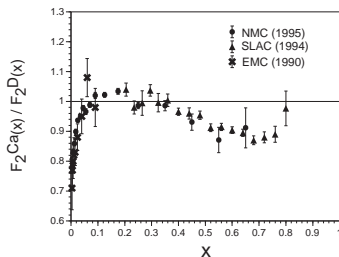


Figure 2.1: Nuclear modification F_2^{Ca}/F_2^D .

$2xF_1 = F_2$. Therefore, we discuss only the F_2 structure function. In parton model, the cross section is described by the incoherent summation of scattering cross sections from individual quarks:

$$F_2(x) = \sum_i e_i^2 x [q_i(x) + \bar{q}_i(x)] \quad . \quad (2.1)$$

We discuss how the structure function F_2 is modified in nuclei. The details of the modification is studied experimentally for several nuclei. For example, SLAC, EMC, and NMC data [5] for the calcium-deuteron F_2 ratio are shown in Fig. 2.1. In the medium x region ($x \sim 0.5$), the ratios are approximately 10% smaller than unity, and it tends to increase at large $x(> 0.8)$. In the region $x \approx 0.2$, the modification is positive,

and the phenomenon is called “antishadowing” in contrast with shadowing at small x . The shadowing part is discussed in section 3.

In describing nuclear structure functions, convolution formalism is usually used. A parton distribution in a nucleus is given by a hadron (nucleon, pion, and etc.) momentum distribution convoluted with a parton distribution in the hadron. In terms of light-cone momenta, it is written as

$$f_{a/A}(x_A, Q^2) = \sum_T \int_{x_A}^1 dy_A f_{a/T}(x_A/y_A, Q^2) f_{T/A}(y_A) \quad , \quad (2.2)$$

where x_A is defined by $x_A = Q^2/2M_A\nu$ and y_A is the light-cone momentum fraction $y_A = p_T^+/p_A^+$. In order to explain the modification of the quark distribution in a nucleus $[f_{a/A}(x_A, Q^2)]$, we may ascribe it to modification of the quark distribution in a hadron $[f_{a/T}(x_A/y_A)]$ or to modification of the hadron distribution in the nucleus $[f_{T/A}(y_A)]$.

A standard approach in describing nuclei in the low-energy region is to start from information on nucleon-nucleon interactions, which are obtained by NN scattering experiments and deuteron properties. Then, the knowledge is applied to nuclear structure by taking into account many-body corrections. In this sense, it is a “proper” approach to start from an assumption that the structure function F_2 of a bound nucleon is the same as the free nucleon F_2 . This way of interpreting the EMC effect is a nuclear binding model [2]. A nuclear tensor, which appears in calculating a lepton-nucleus cross section, is given by the convolution: $W_{\mu\nu}^A(P, q) = \int d^4p S(p) W_{\mu\nu}^N(p, q)$. The spectral function $S(p)$ is the nucleon momentum distribution in the nucleus. If we consider the simplest case of a shell model, it is given by single particle wave functions and binding energies of nucleons: $S(p) = \sum_i |\phi_i(\vec{p})|^2 \delta(p_0 - m_N - \epsilon_i)$. Recoil energy is neglected in the expression. From these equations, the nuclear F_2 is

$$F_2^A(x, Q^2) = \sum_i \int dz f_i(z) F_2^N(x/z, Q^2) \quad , \quad (2.3)$$

where x is the Bjorken variable $x = Q^2/2m_N\nu$, and $f_i(z)$ is the light-cone momentum distribution of the nucleon i :

$$f_i(z) = \int d^3p \, z \, \delta\left(z - \frac{p \cdot q}{m_N\nu}\right) |\phi_i(\vec{p})|^2 \quad . \quad (2.4)$$

The momentum fraction z is given by $z = p \cdot q / m_N\nu = 1 - |\epsilon_i|/m_N + \vec{p} \cdot \vec{q} / m_N\nu \approx 1.00 - 0.02 \pm 0.2$ for a typical nucleon. So, the function $f(z)$ is peaked at 0.98. If we replace $f(z)$ by a delta function $\delta(z - 0.98)$ for simplicity, the nuclear F_2 becomes $F_2^A(x, Q^2) \approx F_2^N(x/0.98, Q^2)$. For example at $x=0.60$, we have $F_2^N(x=0.61)/F_2^N(x=0.60) = 0.88$ and the 10% EMC effect can be explained at medium x .

On the other hand, there exist other extreme interpretations in terms of modification of nucleon itself. A well known idea is the Q^2 rescaling model. It seems that the

nucleon modification makes sense if we consider that the average nucleon separation in a nucleus is about 2 fm, which is almost equal to the nucleon diameter. Therefore, it is no wonder that multi-quark systems other than the nucleon are formed. If such multi-quark hadrons are created, a confinement size for quarks should be changed. Then the quark momentum distributions are modified according to the size change. Using this kind of simple picture at a hadronic scale μ^2 , we calculate distributions at large Q^2 , where experimental data are taken, by evolving distributions from μ^2 . We find that a nuclear F_2 is related to the nucleon one simply by scaling Q^2 :

$$F_2^A(x, Q^2) = F_2^N(x, \xi_A Q^2) \quad , \quad (2.5)$$

with the rescaling parameter $\xi_A = (\lambda_A^2/\lambda_N^2)^{\alpha_s(\mu_A^2)/\alpha_s(Q^2)}$, where λ is the confinement radius for a quark.

The binding and rescaling models seem very different interpretations. How shall we understand the situation? A possible explanation is in terms of factorization scale independence [3]. For example in the operator-product-expansion case, the renormalization scale μ separates long-distance physics and short-distance one. However, final results should not depend on the arbitrary human factor μ . Because the bound structure function and the nucleon momentum distribution are *not* separately observables, the same discussion could be valid in our case. The nuclear structure function, which is a physics observable, should not depend on a factorization scale μ which separates it into the quark-distribution part and the hadron-distribution one. Choosing a nuclear-dependent scale $\mu = \mu_A$, we obtain the rescaling model. On the other hand, the binding model corresponds to the nuclear-independent scale. Using this factorization-scale independence, we may relate the two different descriptions. Moments of a nonsinglet distribution are written as $M_n^{q/A} = M_n^{q/N} M_n^{N/A}$ by Mellin-transformation properties. As a simple example of the binding model, a Fermi-gas model is employed. Relations between the two descriptions are found as $\bar{\epsilon}/m_N = -\gamma_2^{NS} \kappa_A/2\beta_0$ and $k_F^2/m_N^2 = 5(2\gamma_2^{NS} - \gamma_3^{NS})\kappa_A/2\beta_0 + O(\bar{\epsilon}^2/m_N^2)$, where κ_A is defined by $1 - \kappa_A = \alpha_s(\xi_A Q^2)/\alpha_s(Q^2)$. The quantities $\bar{\epsilon}$ and k_F are the average binding energy and the Fermi momentum, and γ_n^{NS} is the nonsinglet anomalous dimension. There exists a correspondence between the binding model and the rescaling, so that we may view the rescaling as an effective description of nuclear medium effects. In fact, it is shown in a simple quark model that effects of nucleon interactions could be effectively described by a nucleon size change in the nuclear medium [6], although it is perhaps too simple to explain various nuclear phenomena. Comparison of the rescaling results with the data is discussed in section 3.

3 Nuclear shadowing

Nuclear modification of F_2 at small x is negative as shown in Fig. 2.1, and it is known as shadowing phenomena. A traditional way of describing the shadowing is in terms

of vector-meson-dominance (VMD) model. The virtual photon transforms into vector meson states, which interact with the target. Because a propagation length of the vector mesons is given by $\lambda = 1/|E_V - E_\gamma| \approx 0.2/x$ fm, it exceeds 2 fm at $x < 0.1$ and multiple scattering occurs. The vector mesons interact predominantly in the surface region, and internal nucleons are “shadowed” by the surfaces ones. This description is not enough for explaining observed small Q^2 dependence. So various extensions of this model are studied. For example, including $q\bar{q}$ continuum, we have the nuclear F_2 [7]

$$F_2^A(x, Q^2) = \frac{Q^2}{\pi} \int dM^2 \frac{M^2 \Pi(M^2)}{(M^2 + Q^2)^2} \sigma_{VA} \quad , \quad (3.1)$$

where σ_{VA} is the vector-meson nucleus interaction cross section, and $\Pi(M^2)$ is the spectral function $\Pi(M^2) = \sigma(e^+e^- \rightarrow \text{hadrons})/\sigma(e^+e^- \rightarrow \mu^+\mu^-) = \text{vector mesons} + q\bar{q} \text{ continuum}$.

Another interpretation of shadowing is in term of Pomeron exchange [8]. In the case of diffractive scattering, the target is thought to be remain intact so that only vacuum quantum number, “Pomeron”, could be exchanged. The Pomeron (\mathcal{P}) structure function is defined by the diffractive cross section: $F_{2,\mathcal{P}} = Q^2/(4\pi^2\alpha)\sigma_{\gamma^*\mathcal{P}}$. Pomeron contribution to the nuclear F_2 from double diffractive scattering is given by a convolution of the Pomeron F_2 with its light-cone momentum distribution: $\delta F_2(x) = \int dy f_{\mathcal{P}}(y) F_{2,\mathcal{P}}(x/y)$. The variable y is the momentum fraction carried by the Pomeron $y = k \cdot q/p \cdot q$. The VMD contribution is compared with the Pomeron result in [9]. Both shadowing results are of the same order of magnitude at small x (≈ 0.01) and at $Q^2=4$ GeV².

The above shadowing ideas are in the target rest frame. There is an explanation in an infinite momentum frame in terms of parton recombinations [10, 11]. Both descriptions are supposedly equivalent; however, there is no explicit proof at this stage. The recombinations are parton interactions from different nucleons. They become dominant at small x with the following reason. The average longitudinal nucleon separation in a Lorentz contracted nucleus is $L = (2 \text{ fm})M_A/P_A = (2 \text{ fm})m_N/p_N$. The longitudinal localization size of a parton with momentum xp_N is $\Delta L = 1/xp_N$. In the x region $x < 0.1$, ΔL becomes larger than L , so that partons from different nucleons could interact significantly. For example, a $p_1 p_2 \rightarrow p_3(x)$ recombination effect on the p_3 parton distribution is

$$\Delta p_3(x) = \frac{9A^{1/3}\alpha_s}{2R_0^2 Q^2} \int dx_1 dx_2 p_1(x_1) p_2(x_2) \Gamma_{p_1 p_2 \rightarrow p_3}(x_1, x_2, x) \delta(x - x_1 - x_2) \quad , \quad (3.2)$$

where the factor $A^{1/3}$ is the number of nucleons in the longitudinal direction, $p_1 p_2 \rightarrow p_3$ cross section is proportional to α_s/Q^2 , and R_0 is given by $R_0 \approx 1$ fm. The parton-fusion function $\Gamma_{p_1 p_2 \rightarrow p_3}$ indicates a probability of the fusion process $p_1 p_2 \rightarrow p_3$. Because it is opposite to the splitting, $\Gamma_{p_1 p_2 \rightarrow p_3}$ is related to the Altarelli-Parisi splitting function by $\Gamma_{p_1 p_2 \rightarrow p_3}(x_1, x_2, x_3) = (x_1 x_2/x_3^2) P_{p_1 \leftarrow p_3}(x_1/x_3) C_{p_1 p_2 \rightarrow p_3}$, where $C_{p_1 p_2 \rightarrow p_3}$ is the

color-factor ratio $C(p_1 p_2 \rightarrow p_3)/C(p_3 \rightarrow p_1 p_2)$. From Eq. (3.2), the recombination shadowing has typical $A^{1/3}$ dependence. Furthermore, the $1/Q^2$ dependence indicates that recombinations are higher-twist effects. Because of this $1/Q^2$ factor, the magnitude of the shadowing depends much on Q^2 at which the recombinations are calculated.

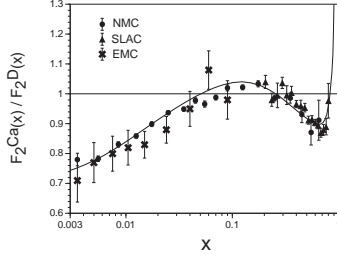


Figure 3.1: Comparison of theoretical results with the data F_2^{Ca}/F_2^D .

As an example of theoretical results, we show the nuclear modification F_2^{Ca}/F_2^D in a model with the recombination and the rescaling mechanisms [11]. Both contributions are calculated at Q_0^2 , then obtained distributions are evolved to the ones at larger Q^2 . The initial point Q_0^2 is considered as a parameter in the model, and it is fixed by fitting the NMC shadowing data for the calcium ($Q_0^2=0.8 \text{ GeV}^2$). The parton distributions at $Q^2=5 \text{ GeV}^2$ are calculated by the DGLAP evolution equations,

and they are compared with the data in Fig. 3.1. Although Q_0^2 is an adjustable parameter, the model can explain the nuclear modification from very small x to large x . It is interesting to note that the antishadowing part at $x \approx 0.2$ is explained by competition between the recombination and the rescaling effects and that the “Fermi motion” part is described by the quark-gluon recombinations.

| | $x < 0.15$ | $x > 0.15$ |
|---------------|------------|------------|
| valence quark | ? | *** |
| sea quark | *** | ** |
| gluon | * ? | * ? |

Table 3.1: Status of nuclear parton distributions.

Current status of nuclear parton distributions are summarized in Table 3.1. The F_2 structure function at medium (small) x is essentially the valence (sea) quark distribution. So we have good information on the valence-quark distribution at medium x and the sea-quark one at small x in several nuclei. The sea-quark distribution is also investigated in Drell-Yan processes. The Fermilab Drell-Yan experiment [12] did not measure the shadowing region as shown in Fig. 3.2. We hope that future measurements at Fermilab and at RHIC probe the shadowing region at very small x . The iron data in Fig. 3.2 are often quoted for concluding that there is little modification in the sea. However, it is not very obvious by looking at other nuclear data. Accurate A dependent data, as well as theoretical studies, are necessary for finding the details of sea-quark behavior. Because the sea-quark distribution dominates F_2 at small x , behavior of valence quarks at small x is not known. However, it could be an interesting topic in testing various shadowing models [13]. The valence-quark shadowing

could be observed by measuring charged pion productions in electron (HERA) or muon scattering.

On the other hand, nuclear gluon distributions are little known. As an example, we show analysis of muon-induced J/ψ production data in a color-singlet model. Obtained gluon ratios in the tungsten and carbon are given in Fig. 3.3 [14]. At this stage, the errors are too large to indicate nuclear modification. Furthermore, the gluon shadowing region is not measured. We hope to have accurate data in future, for example at RHIC.

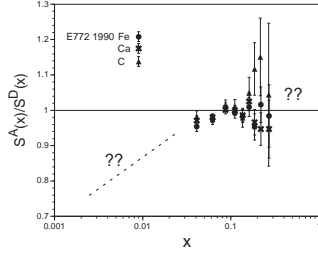


Figure 3.2: Sea-quark distribution in Drell-Yan process.

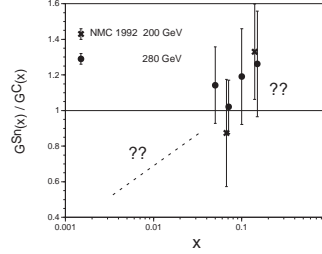


Figure 3.3: Gluon distribution in muon-induced J/ψ production.

4 Nuclear dependence of Q^2 evolution

It is known that the Bjorken scaling, which indicates structure functions are independent of Q^2 , works approximately. Therefore, most studies on the nuclear modification are focused on the x dependence. It is difficult to find small nuclear effects on the scaling violation. However, it became possible to measure such small effects recently [4]. The NMC obtains Q^2 evolution differences in tin and carbon nuclei: $\partial(F_2^{Sn}/F_2^C)/\partial(\ln Q^2)$. It is an interesting topic to investigate whether or not the DGLAP (Dokshitzer-Gribov-Lipatov-Altarelli-Parisi) equations could be applied to nuclear structure functions. In particular, the parton recombinations are predicted to produce higher-twist effects in the evolution [10, 15]:

$$\begin{aligned} \frac{\partial}{\partial t} q_i(x, t) = & \int_x^1 \frac{dy}{y} \left[\sum_j P_{q_i q_j} \left(\frac{x}{y} \right) q_j(y, t) + P_{qg} \left(\frac{x}{y} \right) g(y, t) \right] \\ & + \left(\text{recombination terms} \propto \frac{\alpha_s A^{1/3}}{Q^2} \right) , \end{aligned} \quad (4.1)$$

$$\begin{aligned} \frac{\partial}{\partial t} g(x, t) = & \int_x^1 \frac{dy}{y} \left[\sum_j P_{gq_j} \left(\frac{x}{y} \right) q_j(y, t) + P_{gg} \left(\frac{x}{y} \right) g(y, t) \right] \\ & + \left(\text{recombination terms} \propto \frac{\alpha_s A^{1/3}}{Q^2} \right) , \end{aligned} \quad (4.2)$$

where the variable t is defined by $t = -(2/\beta_0) \ln[\alpha_s(Q^2)/\alpha_s(Q_0^2)]$. The first two terms in Eqs. (4.1) and (4.2) describe the process that a parton p_j with the nucleon's momentum

fraction y splits into a parton p_i with the momentum fraction x and another parton. The splitting function $P_{p_i p_j}(z)$ determines the probability for the parton p_j radiating the parton p_i such that the p_j momentum is reduced by the fraction z . There are additional recombination contributions in Eqs. (4.1) and (4.2).

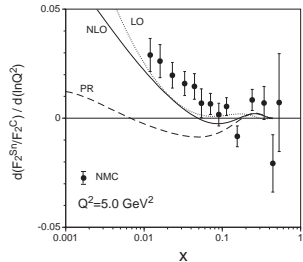


Figure 4.1: Difference of Q^2 evolution in tin and carbon nuclei: $\partial(F_2^{Sn}/F_2^C)/\partial(\ln Q^2)$.

They are evolved to $Q^2=5 \text{ GeV}^2$ by leading-order (LO) DGLAP, next-to-leading-order (NLO) DGLAP, and parton recombination (PR) equations with the help of the computer program `bf1.fort77` in Ref. [15]. The results are compared with the NMC data [4] in Fig. 4.1. The DGLAP evolution curves agree roughly with the experimental data, so that the major nuclear dependence comes from the nuclear modification in the x distributions. The PR evolution curve disagrees with the data; however, it does not mean that the recombination mechanism is ruled out. There are a few uncertain factors. For example, the input higher-dimensional gluon distribution is essentially not known. Further refinement of the recombination contributions to the evolution is necessary. It is nonetheless interesting in the sense that higher-twist effects could be found in studying the nuclear Q^2 evolution.

5 Spin structure of spin-one hadrons

Spin structure of spin-1/2 hadrons has been investigated fairly well. In addition, there is a good possibility to measure a new spin structure function for spin-one hadrons in the near future. As a realistic spin-one target, we have the deuteron. Studying the deuteron spin structure at high energies, we gain an insight into a new aspect of spin physics [17]. There are four new structure functions for spin-one hadrons: b_1 , b_2 , b_3 , and b_4 . In the Bjorken scaling limit, the only relevant structure function is b_1 or equivalently $b_2/2x$. For measuring b_1 , the electron or muon does not have to be polarized but we need polarized deuteron. The b_1 structure function is proportional to the tensor combination of the polarized cross sections: $b_1 \propto d\sigma(0) - [d\sigma(+1) + d\sigma(-1)]/2$. In parton model, it is given by

$$b_1(x) = \sum_i e_i^2 [\delta q_i(x) + \delta \bar{q}_i(x)] \quad , \quad (5.1)$$

where $\delta q_i = [q_i^0 - (q_i^{+1} + q_i^{-1})/2]/2 = \frac{1}{2}[q_i^0(x) - q_i^{+1}(x)]$ with the flavor- i quark distribution $q_i^H(x)$ in z component of the target spin (H). Because quark spin does not appear in the above expression, b_1 probes very different spin structure.

We discuss a sum rule for b_1 [18]. The integral of Eq. (5.1) over x is related to a tensor combination of elastic amplitudes by using the parton picture in an infinite momentum frame. Next, the elastic helicity amplitudes are written by charge and quadrupole form factors of the spin-one hadron. In the case of tensor combination, the charge form factor cancels out and the remaining term is the quadrupole one:

$$\int dx b_1(x) = \lim_{t \rightarrow 0} -\frac{5}{3} \frac{t}{4M^2} F_Q(t) + \frac{1}{9} \delta Q_{sea} \quad , \quad (5.2)$$

where the sea-quark tensor polarization is defined by $\delta Q_{sea} = \int dx [8\delta\bar{u} + 2\delta\bar{d} + \delta s + \delta\bar{s}]$, and $F_Q(t)$ is the quadrupole form factor in the unit of e/M^2 . Equation (5.2) is analogous to the Gottfried integral $\int dx [F_2^p(x) - F_2^n(x)] = 1/3 + (2/3) \int dx [\bar{u}(x) - \bar{d}(x)]$. As the Gottfried sum $1/3$ is obtained by assuming the flavor symmetry $\bar{u} = \bar{d}$, the b_1 sum

$$\int dx b_1(x) = \lim_{t \rightarrow 0} -\frac{5}{3} \frac{t}{4M^2} F_Q(t) = 0 \quad , \quad (5.3)$$

is obtained if there is no sea-quark tensor polarization. Because of this assumption on the tensor polarization, the b_1 sum rule is considered as one of the sum rules in a naive parton model. It is similar to the Gottfried sum rule in this sense. At this stage, all model calculations for $b_1(x)$ satisfy the sum rule $\int dx b_1(x) = 0$. As the breaking of the Gottfried sum rule became an interesting topic recently, it is worth while investigating a possible mechanism to produce the tensor polarization δQ_{sea} , which breaks the sum rule.

Even though the sum-rule value is expected to be zero for the b_1 , it does not mean that b_1 itself is zero. In fact, b_1 can be negative in a certain x region. For example, the deuteron b_1 is given by a helicity amplitude for the nucleon convoluted with a light-like momentum distribution of the nucleon [17, 19]:

$$b_1^D(x) = \int_x^2 \frac{dy}{y} F_1(x/y) \int d^3p \left[-\frac{3}{4\pi\sqrt{2}} \sin\alpha \cos\alpha u_s(p) u_d(p) + \frac{3}{16\pi} \sin^2\alpha u_d^2(p) \right] \\ \times (3\cos^2\theta - 1) \left[1 + \frac{p\cos\theta}{M} + \frac{p^2}{4M^2} \right] \delta \left[y - \frac{p\cos\theta + E(p)}{M} \right] \quad , \quad (5.4)$$

where $\sin\alpha$ is the D-state admixture, and $u_{s,d}$ are S and D-wave deuteron wave functions. The first term is due to the S-D interference and the second to the D-state. This is just an example of nuclear structure aspects. Measured deuteron b_1 does not have to agree with the above estimate. If a deviation from nuclear contributions is found, b_1 provides important clues to physics of non-nucleonic components in nuclei and to new tensor structure on the parton level.

Acknowledgment

This research was partly supported by the Grant-in-Aid for Scientific Research from the Japanese Ministry of Education, Science, and Culture under the contract number 06640406.

* Email: kumanos@cc.saga-u.ac.jp. Information on his research is available at <http://www.cc.saga-u.ac.jp/saga-u/riko/physics/quantum1/structure.html>.

References

- [1] J. J. Aubert et al. (EM Collaboration), Phys. Lett. B 123 (1983) 275.
- [2] S. V. Akulinichev, S. A. Kulagin, and G. M. Vagradov, Phys. Lett. B 158 (1985) 485; S. Kumano and F. E. Close, Phys. Rev. C41 (1990) 1855.
- [3] F. E. Close, R. G. Roberts, and G. G. Ross, Phys. Lett. B129 (1983) 346; Nucl. Phys. B296 (1988) 582.
- [4] Y. Mizuno (NMC), contribution to this conference; A. Mücklich and A. Sandacz, private communications on the preliminary data $\partial[F_2^{S^n}/F_2^C]/\partial[\ln Q^2]$.
- [5] J. Gomez et al. (SLAC-E139), Phys. Rev. D 49 (1994) 4348; M. Arneodo et al. (EMC), Nucl. Phys. B 333 (1990) 1; P. Amaudruz et al. (NMC), Nucl. Phys. B 441 (1995) 3.
- [6] S. Kumano and E. J. Moniz, Phys. Rev. C 37 (1988) 2088.
- [7] G. Piller, W. Ratzka, and W. Weise, Z. Phys. A 352 (1995) 427; L. L. Frankfurt, M. I. Strikman, and S. Liuti, Phys. Rev. Lett. 65 (1990) 1725.
- [8] V. Barone, M. Genovese, N. N. Nikolaev, E. Predazzi, and B. G. Zakharov, Z. Phys. C 58 (1993) 541.
- [9] W. Melnitchouk and A. W. Thomas, Phys. Rev. D 47 (1993) 3783.
- [10] A. H. Mueller and J. Qiu, Nucl. Phys. B268 (1986) 427; F. E. Close, J. Qiu, and R. G. Roberts, Phys. Rev. D40 (1989) 2820.
- [11] S. Kumano, Phys. Rev. C 48 (1993) 2016; C50 (1994) 1247; Phys. Lett. B298 (1993) 171; B342 (1995) 339.
- [12] D. M. Alde et al. (Fermilab-E772), Phys. Rev. Lett. 64 (1990) 2479.
- [13] R. Kobayashi, S. Kumano, and M. Miyama, Phys. Lett. B354 (1995) 465.
- [14] P. Amaudruz et al. (NMC), Nucl. Phys. B371 (1992) 553.
- [15] M. Miyama and S. Kumano, hep-ph/9508246, Comput. Phys. Commun. in press.
- [16] S. Kumano and M. Miyama, hep-ph/9512244, Phys. Lett. B in press.
- [17] P. Hoodbhoy, R. L. Jaffe, and A. Manohar, Nucl. Phys. B312 (1989) 571; L. L. Frankfurt and M. I. Strikman, Nucl. Phys. A405 (1983) 557.
- [18] F. E. Close and S. Kumano, Phys. Rev. D42 (1990) 2377.
- [19] H. Khan and P. Hoodbhoy, Phys. Rev. C44 (1991) 1219.